J. Phys. Chem. 1993, 97, 10977–10983

Thermal Isomerization and Decomposition of 2-Butyne in Shock Waves

Yoshiaki Hidaka,*,† Tetsuo Higashihara,*,‡ Natsuhiko Ninomiya,† Hidekazu Oshita,† and Hiroyuki Kawano†

Department of Chemistry, Faculty of Science, Ehime University, Matsuyama 790, Japan, and Matsue College of Technology, Nishiikuma-cho, Matsue 690, Japan

Received: March 2, 1993; In Final Form: June 14, 1993●

The thermal isomerization and decomposition of 2-C_4H_6 behind reflected shock waves with $1100 < T_5 < 1600$ K and $1.6 \times 10^{-5} < \rho_5 < 2.1 \times 10^{-5}$ mol/cm^3 were studied by UV kinetic absorption spectroscopy, IR laser kinetic absorption spectroscopy, and gas-chromatographic analysis of reaction products. The major products of the pyrolysis were 1,2-butadiene, 1,3-butadiene, CH_4, C_2H_2, C_2H_4, C_2H_6, allene, propyne, C_4H_2, vinylacetylene, and benzene. 1,3-Butadiene and 1,2-butadiene were produced before the appearance of any other decomposition products. This fact means that the very fast isomerizations of 2-butyne take place before the decomposition. The present data were successfully modeled with a 80 reaction mechanism which included the isomerizations among 1- and 2-butynes and 1,2- and 1,3-butadienes and the decompositions of these C_4H_6 isomers. From the modeling, the following rate constants of the isomerizations were obtained: 2-butyne = 1,3-butadiene ($k = (3.0 \times 10^{13}) \exp(-65.0\ \text{kcal}/RT)\ \text{s}^{-1}$), and 2-butyne = 1,2-butadiene ($k = (3.0 \times 10^{13}) \exp(-67.0\ \text{kcal}/RT)\ \text{s}^{-1}$), where the activation energies, 65 and 67 kcal/mol, were estimated from literature data. We discussed the possible route of the isomerizations of 2-butyne to 1,3- and 1,2-butadienes.

Introduction

There are many C_4H_6 isomers such as 1,3-butadiene (1,3-C_4H_6), 1,2-butadiene (1,2-C_4H_6), 1-butyne (1-C_4H_6), 2-butyne (2-C_4H_6), 1-methyl-1-cyclopropene, 3-methyl-1-cyclopropene, cyclobutene, and so on. Among these isomers, the pyrolysis of 1,3-C_4H_6 in shock waves has extensively been studied.[1-4] Kern et al.[5] have studied the thermal decomposition of 1,2-C_4H_6 in shock waves by monitoring reaction products using time-of-flight mass spectrometry. Pyrolysis of other isomers at high temperatures, however, has scarcely been studied.

Among the C_4H_6 isomers, the pyrolytic isomerizations of cyclic compounds such as 1-methyl-1-cyclopropene,[6] cyclobutene,[7] and bicyclo[1.1.0]butane[8,9] to aliphatic isomers have been studied in static reactors. In their study of 1-methyl-1-cyclopropene pyrolysis over the temperature range 483–523 K, Hopf et al.[6] observed the parallel isomerizations of 1-methyl-1-cyclopropene to 2-C_4H_6 (91–94%), 1,3-C_4H_6 (5–8%), and 1,2-C_4H_6 (1–2%). They proposed that these isomers arose via 1,2-H shifts in a diradical-like intermediate (see Scheme I). The isomerizations of aliphatic C_4H_6 isomers, however, have not yet been observed, except for that of 1,2-C_4H_6. In their study of 1,2-C_4H_6 pyrolysis in shock waves, Kern et al.[5] found that, in order to model successfully the C_4H_6 profiles, it was necessary to include the isomerization of 1,2-C_4H_6 to 1,3-C_4H_6.

In this study, we performed a shock tube experiment on the pyrolysis of 2-C_4H_6 using single-pulse, time-resolved IR laser absorption and time-resolved UV absorption methods. We found that 2-C_4H_6 rapidly isomerizes to 1,2-C_4H_6 and 1,3-C_4H_6 before the decomposition of 2-C_4H_6 takes place. We will discuss the mechanism of 2-C_4H_6 isomerization based on the previous study by Hopf et al.[6]

Experimental Section

The test gas compositions used here were 0.4% 2-C_4H_6 in Ar (UV absorption experiment) and 2.5% 2-C_4H_6 in Ar (IR laser absorption and single-pulse experiments). All experiments were done in reflected shock waves over the temperature range 1100–1600 K. Initial sample pressure was kept at 50 Torr, giving reflected shock densities in the range of 1.6×10^{-5} to 2.1×10^{-5} mol/cm^3.

Three shock tubes of 4.1-cm i.d. were used in this experiment. Details of the apparatus and procedures have been described in previous papers.[10-12] The first is a standard-type shock tube connected to a laser absorption apparatus. The transmitted intensities of a 3.39-μm He–Ne laser beam through a 4.1-cm path length in the shock tube and through an interference filter ($\lambda_{max} = 3.39\ \mu$m, half-width = 0.072 μm) were observed with a Judson J10D-M204 InSb detector. The decadic molar extinction coefficients of 2-C_4H_6 at 3.39 μm were computed from the absorbance values at the shock front by assuming that the absorption obeys the Beer–Lambert law. Other hydrocarbons, which would be produced by the pyrolysis of 2-C_4H_6, also absorb at 3.39 μm. The following mixtures were shock heated (more than 20 runs for each mixture) using the same experimental setup as that used in the present study: 1% 1-C_4H_6–99% Ar, 6% 1,3-C_4H_6–94% Ar, 1% 1,2-C_4H_6–99% Ar and 6% 1,2-C_4H_6–94% Ar, 5% C_4H_4–95% Ar, 5% C_3H_6–95% Ar, 4% AC_3H_4–96% Ar, 4% PC_3H_4–96% Ar, 2% C_2H_6–98% Ar and 5% C_2H_6–95% Ar, 6% C_2H_4–94% Ar, 6% C_2H_2–94% Ar, and 5% CH_4–95% Ar. Initial sample pressure of these experiments was kept at 50 Torr. From the absorbance values at the shock front, the decadic molar extinction coefficients of these species were computed by assuming that the absorption of each species obeys the Beer–Lambert law. Between 1200 and 1600 K, the decadic molar extinction coefficients can be approximated as

$$\epsilon(2\text{-}C_4H_6) = (4.995 \times 10^4) - 21.5T\ \text{cm}^2/\text{mol}$$

$$\epsilon(1\text{-}C_4H_6) = (4.40 \times 10^4) - 14T\ \text{cm}^2/\text{mol}$$

$$\epsilon(1,3\text{-}C_4H_6) = (2.35 \times 10^3) + 4.375T\ \text{cm}^2/\text{mol}$$

$$\epsilon(1,2\text{-}C_4H_6) = (2.866 \times 10^4) - 8.786T\ \text{cm}^2/\text{mol}$$

$$\epsilon(C_4H_4) = (-4.924 \times 10^2) + 1.818T\ \text{cm}^2/\text{mol}$$

$$\epsilon(C_3H_6) = (1.064 \times 10^5) - 36T\ \text{cm}^2/\text{mol}$$

$$\epsilon(AC_3H_4) = (2.20 \times 10^3) + 0.44T\ \text{cm}^2/\text{mol}$$

---

† Ehime University.

‡ Matsue College of Technology.

● Abstract published in *Advance ACS Abstracts*, September 15, 1993.

0022-3654/93/2097-10977$04.00/0

$$\epsilon(PC_3H_4) = (1.07 \times 10^4) - 7.75T\ \mathrm{cm^2/mol}$$

$$\epsilon(C_2H_6) = (5.43 \times 10^4) - 17.5T\ \mathrm{cm^2/mol}$$

$$\epsilon(C_2H_4) = 3.375T\ \mathrm{cm^2/mol}$$

$$\epsilon(C_2H_2) = (-1.44 \times 10^3) + 1.025T\ \mathrm{cm^2/mol}$$

$$\epsilon(CH_4) = (3.844 \times 10^4) - 18.7T\ \mathrm{cm^2/mol} \qquad (T < 1500\ \mathrm{K})$$

$$\epsilon(CH_4) = (1.33 \times 10^4) - 2.2T\ \mathrm{cm^2/mol} \qquad (T > 1500\ \mathrm{K})$$

The second is a standard-type shock tube connected to a UV absorption apparatus. The transmitted intensity at 230 nm of a Hamamatsu-L544 D_2 lamp through a 4.1-cm path in the shock tube and through a Rico-MC-20 grating monochromator (half-width = 2.5 nm) was monitored by a Hamamatsu R-306 photomultiplier. The 230-nm light is mainly absorbed by 1,3-C_4H_6. In order to obtain the decadic molar extinction coefficients of 1,3-C_4H_6, 0.1% 1,3-C_4H_6–99.9% Ar (7 runs), and 0.2% 1,3-C_4H_6–99.8% Ar (10 runs), mixtures were shock heated using the same experimental setup as that used in the present study. From the absorbance values at the shock front, the decadic molar extinction coefficients were computed. Other unsaturated hydrocarbons which would be produced by the pyrolysis of 2-C_4H_6 have possibility to absorb the 230 nm light. Then, the following mixtures were shock heated using the same experimental setup as that used in the present study: 2.5% 2-C_4H_6–97.5% Ar (7 runs); 0.4% 1,2-C_4H_6–99.6% Ar (10 runs) and 1% 1,2-C_4H_6–99% Ar (5 runs); 0.75% C_4H_4–99.25% Ar (11 runs); 1% C_4H_2–99% Ar (17 runs); 0.4% C_6H_6–99.6% Ar (7 runs) and 1% C_6H_6–99% Ar (10 runs); 0.5% AC_3H_4–99.5% Ar (10 runs) and 1% AC_3H_4–99% Ar (9 runs); 2% PC_3H_4–98% Ar (10 runs) and 4% PC_3H_4–96% Ar (5 runs); 6% C_2H_4–94% Ar (20 runs); and 6% C_2H_2–94% Ar (9 runs). Initial sample pressure of all the runs was 50 Torr. As before, from the shock front absorbance values, the decadic molar extinction coefficients were computed by assuming that the absorption of each species obeys the Beer–Lambert law. The decadic molar extinction coefficients could be approximated between 1200 and 1600 K as

$$\log(\epsilon(1,3\text{-}C_4H_6)/\mathrm{cm^2\ mol^{-1}}) = 6.74$$

$$\log(\epsilon(1,2\text{-}C_4H_6)/\mathrm{cm^2\ mol^{-1}}) = 5.43$$

$$\log(\epsilon(2\text{-}C_4H_6)/\mathrm{cm^2\ mol^{-1}}) = 4.85$$

$$\log(\epsilon(C_4H_4)/\mathrm{cm^2\ mol^{-1}}) = 6.279$$

$$\log(\epsilon(C_4H_2)/\mathrm{cm^2\ mol^{-1}}) = 5.778$$

$$\log(\epsilon(C_6H_6)/\mathrm{cm^2\ mol^{-1}}) = (1.2 \times 10^{-3})T + 3.84$$

$$\log(\epsilon(AC_3H_4)/\mathrm{cm^2\ mol^{-1}}) = (2.83 \times 10^{-4})T + 4.93$$

$$\log(\epsilon(PC_3H_4)/\mathrm{cm^2\ mol^{-1}}) = (8.0 \times 10^{-4})T + 3.64$$

$$\log(\epsilon(C_2H_4)/\mathrm{cm^2\ mol^{-1}}) = (1.433 \times 10^{-3})T + 2.11$$

$$\log(\epsilon(C_2H_2)/\mathrm{cm^2\ mol^{-1}}) = (4.0 \times 10^{-4})T + 2.86$$

The third is a magic-hole-type shock tube. Within 20 s after shock heating, the reacted gas mixtures were extracted into a preevacuated vessel (50 cm^3) through a valve at 1-cm upstream from the end plate and analyzed on three serially connected gas chromatographs with thermal conductivity detectors. An identification and a quantification of each product were done using the following two mixtures: one is the standard gas sample (0.482% CH_4, 0.514% C_2H_6, 0.514% C_2H_4, 0.464% C_2H_2, 0.482% C_3H_8, 0.476% C_3H_6, 0.482% PC_3H_4, 0.477% AC_3H_4, 0.471% CO, and 0.538% CO_2 diluted with Ar) prepared by Seitetsu Kagaku Co., Ltd., and the other is the mixture of 0.2% C_4H_2, 0.2% C_4H_4, 0.2% 2-C_4H_6, 0.2% 1-C_4H_6, 0.2% 1,2-C_4H_6, 0.2% 1,3-C_4H_6, and 0.2% C_6H_6 diluted with Ar, which was prepared by us manometrically. These mixtures were repeatedly measured on the gas chromatographs, and overall accuracies in the gas chromatographic results were confirmed to be within ±5%. Pressure signals at 1 cm upstream from the end plate were recorded to check the constancy of pressure and to determine an effective heating time. The effective heating time was defined as the time elapsed between the reflected shock front and 80% point of the shock front pressure. The validity of this assumption has already been confirmed.[10] The effective heating times were 2010 μs (1100 K), 1920 μs (1200 K), 1820 μs (1300 K), 1730 μs (1400 K), and 1630 μs (1500 K).

Results

The products of the pyrolysis of 2-C_4H_6 were 1,3-C_4H_6, 1,2-C_4H_6, 1-C_4H_6, CH_4, C_2H_2, C_2H_4, C_2H_6, allene (AC_3H_4), propyne (PC_3H_4), vinylacetylene (C_4H_4), C_4H_2, and benzene (C_6H_6). The yields of these products and remaining reactant were plotted against temperature in Figure 1. From this figure, it is apparent that at low temperatures (up to 1200 K) 1,3-C_4H_6 and 1,2-C_4H_6 are the only products. At around 1200 K, CH_4, propyne, C_4H_4, and 1-C_4H_6 begin to appear. C_2H_4 and C_2H_2 are not formed until 1250 K. These results suggest that 2-C_4H_6 rapidly isomerizes before the decomposition takes place.

Figure 2 shows a typical absorption profile at 230 nm. In Figure 3 are shown $\log(I_f/I_t)$ values at 230 nm against reaction time for three runs, where I_f is the transmitted intensity with no absorption and I_t is the transmitted intensity at time t from the shock front. Slight absorption observed just behind the shock front is due to 2-C_4H_6. The extinction coefficient of 1,3-C_4H_6 is largest. Below 1400 K, almost all absorption at 230 nm is due to 1,3-C_4H_6. It can be seen in Figure 3 that 1,3-C_4H_6 is rapidly produced from the beginning of the reaction.

In order to parametrize the progress of early stage reaction from the IR absorption profiles at 3.39 μm, we measured A_{50}, A_{100}, and A_{200} according to the equation $A_t = \log(I_f/I_t)/\log(I_f/I_0)$, where I_f is the transmitted intensity with no absorption, and I_0 and I_t are the transmitted intensities at the shock front and time t, respectively. These data are plotted against temperature in Figure 4.

Modeling Calculations

We observed a mixture of C_4H_6 isomers in the product mixture as is seen in Figure 1. This fact means that the isomerizations of 2-C_4H_6 occur simultaneously with the decomposition. Four isomerization reactions

$$2\text{-}C_4H_6 = 1,3\text{-}C_4H_6 \qquad \Delta H^\circ_{298} = -8.5\ \mathrm{kcal/mol} \qquad (1)$$

$$2\text{-}C_4H_6 = 1,2\text{-}C_4H_6 \qquad \Delta H^\circ_{298} = 4.0\ \mathrm{kcal/mol} \qquad (2)$$

$$1,2\text{-}C_4H_6 = 1,3\text{-}C_4H_6 \qquad \Delta H^\circ_{298} = -12.5\ \mathrm{kcal/mol} \qquad (3)$$

$$1\text{-}C_4H_6 = 1,2\text{-}C_4H_6 \qquad \Delta H^\circ_{298} = -0.7\ \mathrm{kcal/mol} \qquad (4)$$

were necessary in order to interpret the experimental yields of the C_4H_6 isomers. The possibility of reaction 3 has been suggested by Kern et al.[5] Other isomerization reactions have not yet been reported. Rate constants for reactions 1 and 2 were optimized in this study to be

$$k_1 = (3.0 \times 10^{13}) \exp(-65000\ \mathrm{cal}/RT)\ \mathrm{s^{-1}}$$

$$k_2 = (3.0 \times 10^{13}) \exp(-67000\ \mathrm{cal}/RT)\ \mathrm{s^{-1}}$$

The k_3 and k_4 values were optimized in separate experimental and modeling studies of 1,2-C_4H_6[13] and 1-C_4H_6[14] pyrolysis to be

$$k_3 = (2.5 \times 10^{13}) \exp(-63000\ \mathrm{cal}/RT)\ \mathrm{s^{-1}}$$

$$k_4 = (2.5 \times 10^{13}) \exp(-65000\ \mathrm{cal}/RT)\ \mathrm{s^{-1}}$$

The activation energies of reactions 1–3, 65, 67, and 63 kcal/

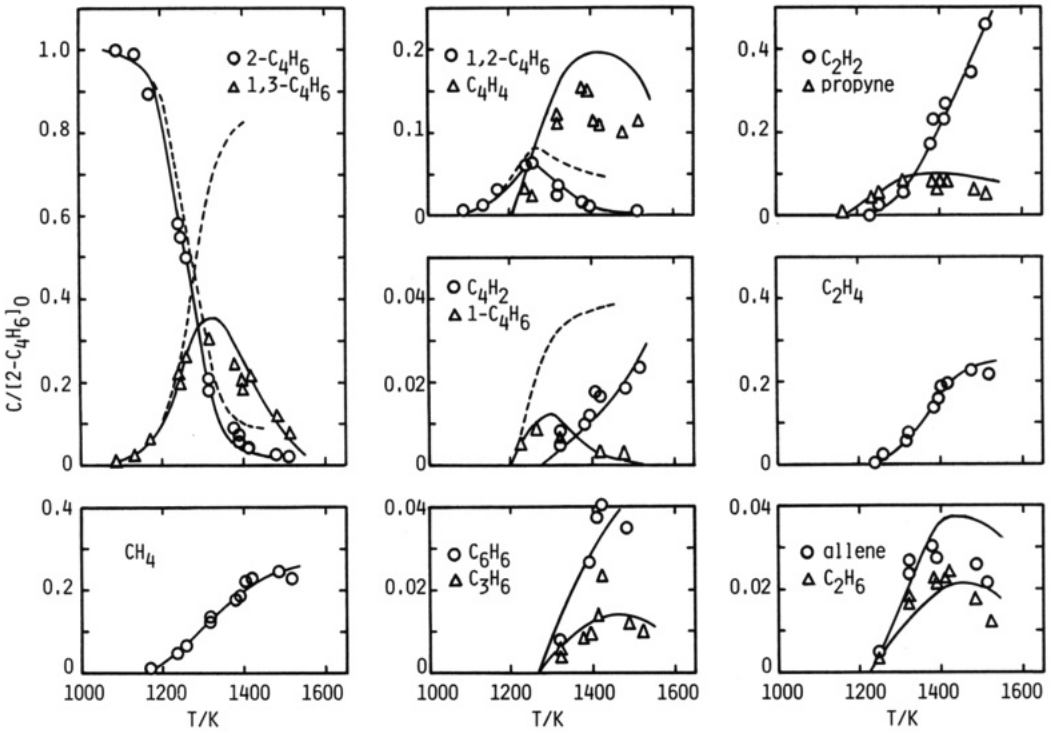

Figure 1. Comparison of experimental (symbols) with computed (lines) product distribution for the 2.5% 2-C_4H_6–97.5% Ar mixture: ——, computed with the Table I mechanism; – – –, computer using only reactions 1–4.

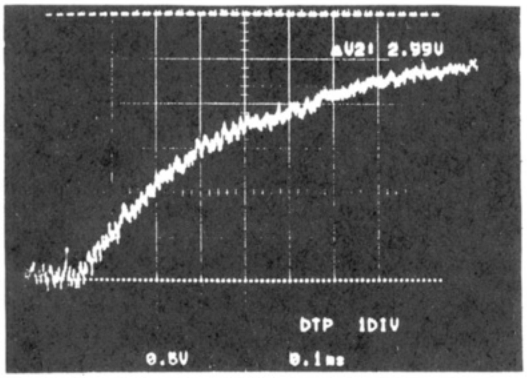

Figure 2. Typical absorption profile at 230 nm: full intensity $I_f = 2.99$ V, signal voltage = 0.5 V/div, sweep time = 100 μs/div. Conditions: 0.4% 2-C_4H_6–99.6% Ar; $P_1 = 50$ Torr; $T_5 = 1352$ K.

mol, were assumed to be nearly equal to the highest barriers of the reactions (see Figure 5). Reaction 4 would proceed in the same manner as the isomerization of propyne to allene proposed by Honjyou et al.[15] An activation energy of 65 kcal/mol was assumed.

Because the decomposition of 2-C_4H_6 is accompanied by the isomerizations, we have to take the decomposition reactions of the four C_4H_6 isomers into account. Initially, C–C single bond fissions and C–H bond fissions were considered for all the isomers. From modeling calculations, however, the following two C–C single bond fissions were found to be dominant:

$$1,2\text{-}C_4H_6 = C_3H_3 + CH_3 \qquad \Delta H^\circ_{298} = 77.8\ \text{kcal/mol} \quad (6)$$

$$1\text{-}C_4H_6 = C_3H_3 + CH_3 \qquad \Delta H^\circ_{298} = 77.1\ \text{kcal/mol} \quad (7)$$

Rate constants for reactions 6 and 7 were optimized in separate experiments[13,14] as

$$k_6 = (2.0 \times 10^{15}) \exp(-75000\ \text{cal}/RT)\ \text{s}^{-1}$$

$$k_7 = (3.0 \times 10^{15}) \exp(-75800\ \text{cal}/RT)\ \text{s}^{-1}$$

The activation energy of reaction 6, 75 kcal/mol, was assumed to be slightly lower than the heat of reaction. The activation energy of reaction 7, 75.8 kcal/mol, was adopted from the high-pressure-limit rate constant expression proposed by Dean,[16] $k_{7,\infty} = (5.0 \times 10^{15}) \exp(-75800\ \text{cal}/RT)\ \text{s}^{-1}$. Other C–C single bond fissions and C–H bond fissions

$$2\text{-}C_4H_6 = 2\text{-}C_4H_5 + H \qquad \Delta H^\circ_{298} = 89.6\ \text{kcal/mol} \quad (5)$$

$$k_5 = (5.0 \times 10^{14}) \exp(-87300\ \text{cal}/RT)\ \text{s}^{-1} \quad (\text{ref } 16)$$

$$2\text{-}C_4H_6 = CH_3C{\equiv}C^\bullet + CH_3 \qquad \Delta H^\circ_{298} = 123.0\ \text{kcal/mol} \quad (\text{a}1)$$

$$k_{a1} = (1.00 \times 10^{17}) \exp(-120000\ \text{cal}/RT)\ \text{s}^{-1}\ (\text{assumed})$$

$$1,3\text{-}C_4H_6 = C_2H_3 + C_2H_3 \qquad \Delta H^\circ_{298} = 117.1\ \text{kcal/mol} \quad (\text{a}2)$$

$$k_{-a2} = 7.22 \times 10^{13}\ \text{cm}^3\ \text{mol}^{-1}\ \text{s}^{-1} \quad (\text{ref } 17)$$

$$1\text{-}C_4H_6 = 1\text{-}IC_4H_5 + H \qquad \Delta H^\circ_{298} = 86.6\ \text{kcal/mol} \quad (\text{a}3)$$

$$k_{a3} = (7.0 \times 10^{14}) \exp(-86000\ \text{cal}/RT)\ \text{s}^{-1}\ (\text{assumed})$$

$$1,2\text{-}C_4H_6 = 1,2\text{-}C_4H_5 + H \qquad \Delta H^\circ_{298} = 85.5\ \text{kcal/mol} \quad (\text{a}4)$$

$$k_{a4} = (6.3 \times 10^{14}) \exp(-85900\ \text{cal}/RT)\ \text{s}^{-1} \quad (\text{ref } 16)$$

$$1,3\text{-}C_4H_6 = 1,3\text{-}IC_4H_5 + H \qquad \Delta H^\circ_{298} = 98.0\ \text{kcal/mol} \quad (\text{a}5)$$

$$k_{a5} = (7.0 \times 10^{14}) \exp(-95000\ \text{cal}/RT)\ \text{s}^{-1}\ (\text{assumed})$$

had negligible effect on the computed results, as long as we used the rate constants given above. For the decomposition of 1,3-C_4H_6, the possibility of a molecular elimination reaction

$$1,3\text{-}C_4H_6 \rightarrow H_2C_2{:} + C_2H_4 \rightarrow C_2H_2 + C_2H_4 \quad (8)$$

has been suggested.[3,4] We included this reaction in our mechanism. The rate constant used for this reaction was that optimized in our experimental and modeling study[18] of 1,3-C_4H_6 pyrolysis,

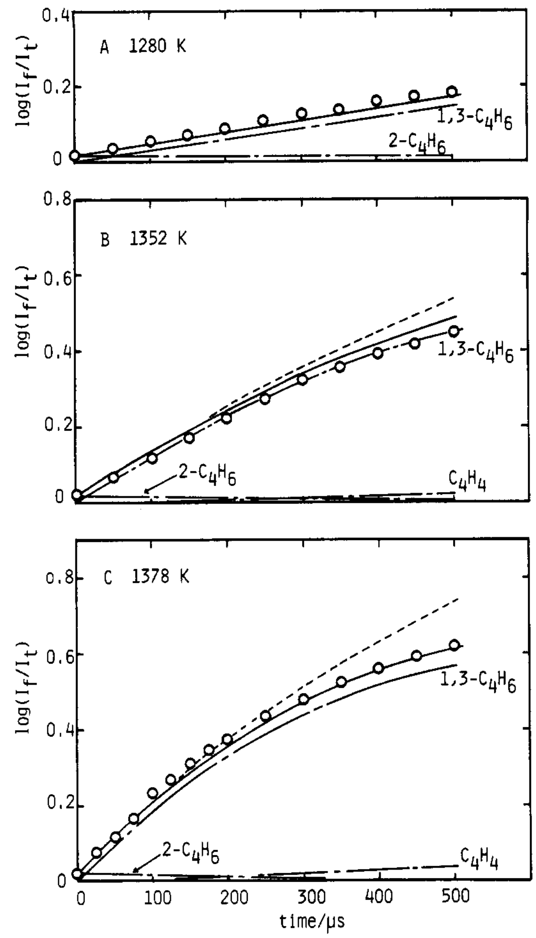

Figure 3. Comparison of experimental (O) with computed (lines) UV absorption profiles at 230 nm for the 0.4% 2-C_4H_6 mixture: (A) P_1 = 50 Torr, T_5 = 1280 K; (B) P_1 = 50 Torr, T_5 = 1352 K; (C) P_2 = 50 Torr, T_5 = 1378 K; (——) computed with the Table I mecahnism, (– – –) computed using only reactions 1–4, (– · –) absorption due to 2-C_4H_6, 1,3-C_4H_6, and C_4H_4.

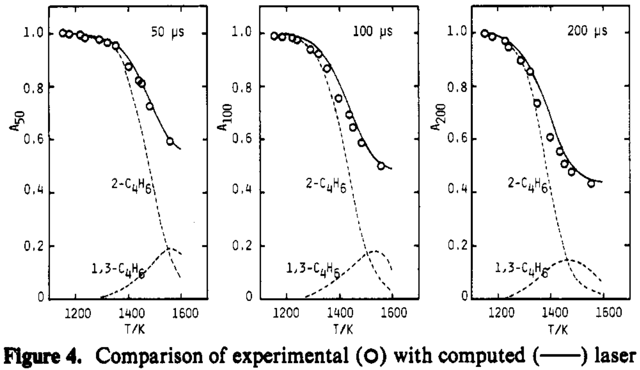

Figure 4. Comparison of experimental (O) with computed (——) laser absorption data, A_t, for the 2.5% 2-C_4H_6–97.5% Ar mixture at 50, 100, and 200 μs. Initial sample pressure, P_1, is 50 Torr. Broken lines represent absorption due to 2-C_4H_6 and 1,3-C_4H_6.

$k_8 = (1.0 \times 10^{14}) \exp(-75000\ \mathrm{cal}/RT)\ \mathrm{s}^{-1}$. This value is about half of that derived by Kiefer et al.;[4] $k_8 = (2.6 \times 10^{15}) \exp(-82500\ \mathrm{cal}/RT)\ \mathrm{s}^{-1}$.

As secondary reactions, the following reactions were found to be important: H atom addition to C_4H_6 isomers and subsequent decomposition of the adducts (reactions 10–14), H atom abstraction from C_4H_6 isomers by H, CH_3, and C_2H_3 (reactions 15–30), and subsequent decomposition of the C_4H_5 isomers (reactions 35–42). Rate constants for these secondary reactions were assumed, when rate constant expressions were not available. We also added reactions which describe the formation and consumption of the products such as CH_4, C_2H_2, C_2H_4, C_2H_6, allene, propyne, C_4H_2, C_4H_4, and benzene.

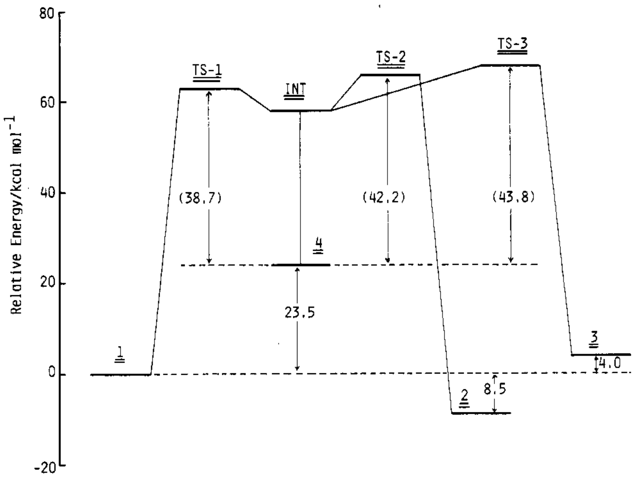

Figure 5. Energy diagram for the isomerizations of 2-C_4H_6 (**1**) to 1,3-C_4H_6 (**2**) and 1,2-C_4H_6 (**3**). Energies in parentheses are the activation energies proposed by Hopf et al.[6] for the isomerizations of 1-methyl-1-cyclopropene (**4**) to 2-C_4H_6, 1,3-C_4H_6, and 1,2-C_4H_6.

In Table I are shown the final mechanism and the rate constants used to interpret the present data. Reverse reactions were automatically included in a computer program through equilibrium constants computed from polynomial fits to standard thermochemical data. Thermochemical data of C_4H_6 isomers and C_4H_5 isomers used in this study are presented in Table II. The thermochemical data of C_4H_5 isomers were estimated by using group additivity methods.[28] For other species we used the same thermochemical data as those used in previous papers.[10–12] The heat of formation of C_2H_3 reported so far ranges from 63 to 77 kcal/mol. We used the value of $\Delta H^\circ_{f,298}$ = 71.7 kcal/mol, which is determined experimentally by Ervin et al.[30] and theoretically by Wu and Carter.[31] Solid lines in Figures 1, 3, and 4 are the results computed using the rate constant set listed in Table I. As are seen in these figures, the present experimental data are satisfactorily modeled by the mechanism and the rate constant set listed in Table I. In Figures 1 and 3 are also shown by broken lines the results computed using only reactions 1–4. Under 1250 K, the yields of 1,3-C_4H_6 and 1,2-C_4H_6 and remaining 2-C_4H_6 can well be explained by reactions 1–4. The UV absorption profiles are also reproduced by reactions 1–4. These facts imply that 2-C_4H_6 is mainly consumed by the isomerizations.

Discussion

Mechanism of 2-C_4H_6 Isomerization. It is apparent, from both the experimental results and the modeling calculations, that 2-C_4H_6 rapidly isomerizes to 1,2-C_4H_6 and 1,3-C_4H_6. These isomerizations can well be explained by the mechanism proposed by Hopf et al.[6] for the isomerizations of 1-methyl-1-cyclopropene to 2-C_4H_6, 1,3-C_4H_6, and 1,2-C_4H_6 (Scheme I). Their mechanism of 1-methyl-1-cyclopropene isomerization is as follows: the first step is the ring opening to produce diradical (INT in Scheme I), and the second step is 1,2-H shifts (TS-1, TS-2, and TS-3 in Scheme I) to produce stable C_4H_6 isomers. According to their mechanism, the isomerization of 2-C_4H_6 would proceed as follows: the first step is 1,2-H shift to produce diradical intermediate (INT) via TS-1, and the second step is another 1,2-H shift to produce 1,3-C_4H_6 and 1,2-C_4H_6 via TS-2 and TS-3. Figure 5 shows an energy diagram for the isomerizations of 2-C_4H_6. The energies given in parentheses, 38.7, 42.2, and 43.8 kcal/mol, are the activation energies proposed by Hopf et al. for the isomerizations of 1-methyl-1-cyclopropene to 2-C_4H_6, 1,3-C_4H_6, and 1,2-C_4H_6. Because their experiments were performed in the high-pressure limit (at least within 2%), these activation energies will be close to the energy barriers of these isomerizations. From these energy barriers and the differences of the standard

TABLE I. Reaction Mechanism and Rate Constant Expression[a]

eq no.	reaction	*A*	*n*	E_a	ref
1	2-C_4H_6 = 1,3-C_4H_6	3.00E+13	0.0	65.0	this work
2	2-C_4H_6 = 1,2-C_4H_6	3.00E+13	0.0	67.0	this work
3	1,2-C_4H_6 = 1,3-C_4H_6	2.50E+13	0.0	63.0	13
4	1-C_4H_6 = 1,2-C_4H_6	2.50E+13	0.0	65.0	14
5	2-C_4H_6 = 2-C_4H_5 + H	5.00E+14	0.0	84.0	16
6	1,2-C_4H_6 = C_3H_3 + CH_3	2.00E+15	0.0	75.0	13
7	1-C_4H_6 = C_3H_3 + CH_3	3.00E+15	0.0	75.8	14
8	1,3-C_4H_6 = C_2H_4 + C_2H_2	1.00E+14	0.0	75.0	18
9	1,3-C_4H_6 = C_4H_4 + H_2	2.00E+13	0.0	75.0	18
10	2-C_4H_6 + H = CH_3 + PC_3H_4	2.60E+05	2.5	1.0	=2k_{58}(assumed)
11	1,3-C_4H_6 + H = C_2H_3 + C_2H_4	2.00E+13	0.0	5.0	18
12	1,2-C_4H_6 + H = CH_3 + AC_3H_4	6.00E+12	0.0	2.1	=(3/4)k_{55}(assumed)
13	1-C_4H_6 + H = CH_3 + AC_3H_4	1.30E+05	2.5	1.0	=k_{58}(assumed)
14	1-C_4H_6 + H = C_2H_5 + C_2H_2	6.50E+04	2.5	1.0	=(1/2)k_{58}(assumed)
15	2-C_4H_6 + H = 2-C_4H_5 + H_2	1.30E+14	0.0	9.4	=k_{64}(assumed)
16	1,3-C_4H_6 + H = 1,3-NC_4H_5 + H_2	5.00E+15	0.0	22.8	=k_{67}(assumed)
17	1,3-C_4H_6 + H = 1,3-IC_4H_5 + H_2	2.50E+15	0.0	22.8	=(1/2)k_{67}(assumed)
18	1,2-C_4H_6 + H = 1,2-C_4H_5 + H_2	6.50E+13	0.0	9.4	=(1/2)k_{64}(assumed)
19	1-C_4H_6 + H = 1-IC_4H_5 + H_2	6.50E+13	0.0	9.4	=(1/2)k_{64}(assumed)
20	1-C_4H_6 + H = 1-NC_4H_5 + H_2	6.50E+13	0.0	9.4	=(1/2)k_{64}(assumed)
21	2-C_4H_6 + CH_3 = 2-C_4H_5 + CH_4	2.00E+14	0.0	19.5	=4k_{63}(adjusted)
22	1,3-C_4H_6 + CH_3 = 1,3-NC_4H_5 + CH_4	4.00E+14	0.0	22.8	=(1/12.5)k_{67} (assumed)
23	1,3-C_4H_6 + CH_3 = 1,3-IC_4H_5 + CH_4	2.00E+14	0.0	22.8	=(1/25)k_{67} (assumed)
24	1,2-C_4H_6 + CH_3 = 1,2-C_4H_5 + CH_4	1.00E+14	0.0	19.5	=2k_{63}(assumed)
25	1-C_4H_6 + CH_3 = 1-IC_4H_5 + CH_4	1.00E+14	0.0	19.5	=2k_{63}(assumed)
26	1-C_4H_6 + CH_3 = 1-NC_4H_5 + CH_4	1.00E+14	0.0	19.5	=2k_{63}(assumed)
27	2-C_4H_6 + C_2H_3 = 2-C_4H_5 + C_2H_4	1.50E+13	0.0	10.0	=k_{62}(assumed)
28	1,3-C_4H_6 + C_2H_3 = 1,3-NC_4H_5 + C_2H_4	5.00E+14	0.0	22.8	=(1/10)k_{67} (assumed)
29	1,2-C_4H_6 + C_2H_3 = 1,2-C_4H_5 + C_2H_4	7.50E+12	0.0	10.0	=(1/2)k_{62}(assumed)
30	1-C_4H_6 + C_2H_3 = 1-NC_4H_5 + C_2H_4	1.50E+13	0.0	10.0	=k_{62}(assumed)
31	2-C_4H_6 + C_3H_3 = 2-C_4H_5 + AC_3H_4	1.00E+13	0.0	19.5	=(1/5)k_{63}(assumed)
32	1,3-C_4H_6 + C_3H_3 = 1,3-NC_4H_5 + AC_3H_4	1.00E+13	0.0	22.5	5
33	1,2-C_4H_6 + C_3H_3 = 1,2-C_4H_5 + AC_3H_4	5.00E+12	0.0	19.5	=(1/10)k_{63} (assumed)
34	1-C_4H_6 + C_3H_3 = 1-NC_4H_5 + AC_3H_4	1.00E+13	0.0	19.5	=(1/5)k_{63}(assumed)
35	2-C_4H_5 = C_4H_4 + H	3.00E+13	0.0	45.0	assumed
36	1,3-IC_4H_5 = C_4H_4 + H	5.00E+13	0.0	44.0	assumed
37	1,3-NC_4H_5 = C_2H_3 + C_2H_2	5.00E+13	0.0	43.9	1/2 of ref 16
38	H + C_4H_4 = 1,3-NC_4H_5	4.00E+13	0.0	3.0	12
39	1,2-C_4H_5 = C_4H_4 + H	3.00E+13	0.0	45.0	assumed
40	1-IC_4H_5 = C_4H_4 + H	3.00E+13	0.0	45.0	assumed
41	1-NC_4H_5 = C_4H_4 + H	3.00E+13	0.0	45.0	assumed
42	1-NC_4H_5 = C_2H + C_2H_4	2.00E+14	0.0	57.0	assumed
43	C_4H_4 = C_2H_2 + C_2H_2	3.40E+13	0.0	77.1	12
44	C_4H_4 + H = IC_4H_3 + H_2	1.00E+07	2.0	6.0	12
45	C_4H_4 + H = NC_4H_3 + H_2	5.00E+06	2.0	6.0	12
46	C_4H_4 + H = C_2H_3 + C_2H_2	1.00E+13	0.0	3.6	12
47	IC_4H_3 + M = C_4H_2 + H + M	3.20E+15	0.0	45.0	12
48	NC_4H_3 + M = C_4H_2 + H + M	6.30E+15	0.0	45.0	12
49	NC_4H_3 = C_2H_2 + C_2H	3.20E+14	0.0	57.2	16
50	C_2H_2 + C_2H = C_4H_2 + H	9.03E+13	0.0	0.0	19
51	C_4H + H_2 = C_4H_2 + H	2.00E+13	0.0	0.0	12
52	C_3H_6 = C_2H_3 + CH_3	8.00E+14	0.0	88.0	20
53	C_3H_6 = CH_4 + C_2H_2	3.50E+12	0.0	70.0	20
54	C_3H_6 + H = C_3H_5 + H_2	1.80E+13	0.0	1.5	20
55	AC_3H_4 + H = C_3H_5	8.00E+12	0.0	2.1	20
56	PC_3H_4 + M = C_3H_3 + H + M	4.70E+18	0.0	80.0	10
57	PC_3H_4 + CH_3 = C_3H_3 + CH_4	2.00E+12	0.0	7.7	10
58	PC_3H_4 + H = C_2H_2 + CH_3	1.30E+05	2.5	1.0	10
59	AC_3H_4 = PC_3H_4	2.50E+12	0.0	59.0	10
60	AC_3H_4 + M = C_3H_3 + H + M	2.00E+18	0.0	80.0	10
61	C_2H_6 = CH_3 + CH_3	7.00E+14	0.0	80.0	21
62	C_2H_6 + C_2H_3 = C_2H_5 + C_2H_4	1.50E+13	0.0	10.0	21
63	C_2H_6 + CH_3 = C_2H_5 + CH_4	5.00E+13	0.0	19.5	21
64	C_2H_6 + H = C_2H_5 + H_2	1.30E+14	0.0	9.4	21
65	CH_3 + CH_3 = C_2H_5 + H	2.80E+13	0.0	13.6	22
66	C_2H_5 = C_2H_4 + H	1.20E+12	0.0	35.0	21
67	C_2H_4 + H = C_2H_3 + H_2	5.00E+15	0.0	22.8	23
68	C_2H_3 + M = C_2H_2 + H + M	7.90E+14	0.0	31.5	24
69	C_2H + H_2 = C_2H_2 + H	1.08E+13	0.0	2.2	19
70	CH_4 + H = CH_3 + H_2	7.20E+14	0.0	15.1	21
71	1,3-NC_4H_5 + C_2H_2 = C_6H_6 + H	1.00E+13	0.0	0.0	12
72	NC_4H_3 + C_2H_2 = C_6H_5	1.00E+13	0.0	0.0	12
73	C_2H + C_4H_2 = C_6H_2 + H	4.00E+13	0.0	0.0	12
74	C_4H + C_2H_2 = C_6H_2 + H	4.00E+13	0.0	0.0	12
75	C_3H_3 + C_3H_3 = C_6H_6	3.00E+12	0.0	0.0	13, 14
76	C_3H_3 + C_3H_3 = C_6H_5 + H	6.00E+13	0.0	10.0	assumed
77	C_6H_6 = C_6H_5 + H	5.00E+15	0.0	107.9	25
78	C_6H_6 + H = C_6H_5 + H_2	2.51E+14	0.0	16.0	26
79	C_6H_5 + C_2H_2 = C_8H_6 + H	1.00E+13	0.0	0.0	12
80	C_6H_5 + C_6H_5 = $C_{12}H_{10}$	3.00E+12	0.0	0.0	27

[a] Rate constants are given in the form, $k = AT^n \exp(-E_a/RT)$. The units are cm, mol, kcal, s, and K. Species identification: IC_4H_3, $CH{\equiv}C{-}\dot{C}{=}CH_2$ radical; NC_4H_3, $CH{\equiv}C{-}CH{=}\dot{C}H$ radical; C_6H_5, phenyl radical; C_8H_6, phenyl acetylene; $C_{12}H_{10}$, biphenyl; structures of C_4H_5 isomers are shown in Table II.

TABLE II: Thermochemical Parameters of C_4H_6 Isomers and C_4H_5 Isomers

name	structure	$\Delta H^\circ_{f,298}$	S°_{298}	C_p°				
				298 K	500 K	800 K	1000 K	1500 K
2-C_4H_6[a]	$CH_3{-}C{\equiv}C{-}CH_3$	34.75	67.66	18.63	26.36	35.13	39.20	45.77
1-C_4H_6[a]	$CH{\equiv}C{-}CH_2{-}CH_3$	39.48	69.50	19.46	27.63	35.95	39.82	46.22
1,2-C_4H_6[a]	$CH_2{=}C{=}CH{-}CH_3$	38.79	69.98	19.15	27.39	36.02	40.01	46.20
1,3-C_4H_6[a]	$CH_2{=}CH{-}CH{=}CH_2$	26.27	66.62	19.11	28.51	36.83	40.51	46.34
2-C_4H_5[b]	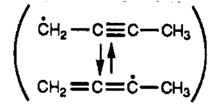	72.3 (74.3)	71.2	18.7	25.8	33.0	36.4	41.6
1-IC_4H_5[b]	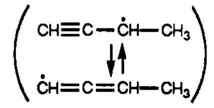	74.0 (75.9)	71.2	18.9	26.1	33.3	36.6	41.7
1-NC_4H_5[b]	$CH{\equiv}C{-}CH_2{-}\dot{C}H_2$	85.6	72.8	18.1	25.6	32.8	36.2	41.6
1,3-NC_4H_5[c]	$\dot{C}H{=}CH{-}CH{=}CH_2$	82.6 (86.5)	69.1	18.6	23.8	31.6	36.7	41.8
1,3-IC_4H_5[b]	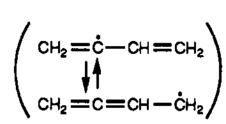	72.2 (74.1)	69.9	18.5	26.5	34.3	37.8	42.9
1,2-C_4H_5[b]								

[a] *Handbook of Chemistry*, 3rd ed.; Ed. by the Chemical Society of Japan: Maruzen: Tokyo, 1984; Chapter 9. [b] Estimated using group additivity methods.[28] We used the values of $\Delta H^\circ_{f,298}[\dot{C}{-}(H)_2(C_t)] = 27.3$ kcal/mol and $\Delta H^\circ_{f,298}[\cdot C{-}(H)(C)(C_t)] = 29.6$ kcal/mol, which were derived from the propargyl resonance energy of 8.6 kcal/mol.[29] [c] Weissman, M.; Benson, S. W. *Int. J. Chem. Kinet.* **1984**, *16*, 307. Units are kcal/mol for the heats of formation and cal K^{-1} mol^{-1} for the entropies and heat capacities. The heats of formation given in parentheses are the BAC–MP4 results by Miller and Melius (Miller, J. A.; Melius, C. F. *Combust. Flame* **1992**, *91*, 21).

SCHEME I

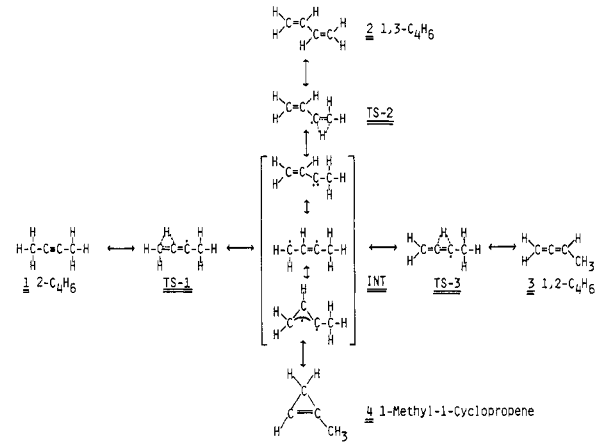

heats of formation of the C_4H_6 isomers, we estimated the barriers of 2-C_4H_6 isomerizations to 1,3-C_4H_6 and 1,2-C_4H_6 to be 65.7 kcal/mol (TS-2) and 67.3 kcal/mol (TS-3), respectively. We tentatively adopted 65 and 67 kcal/mol as the activation energies (E_{a_1} and E_{a_2}) of reactions 1 and 2. Although these activation energies can well explain our experimental results, computed results are not so sensitive to the choice of E_{a_1} and E_{a_2}. Variations of E_{a_1} and E_{a_2} by 5 kcal/mol impair the fits only slightly, as long as the absolute values of k_1 and k_2 remain the same at 1300 K. However, variations of E_{a_1} and E_{a_2} by 10 kcal/mol make the fits worse, especially when E_{a_1} and E_{a_2} were enlarged.

Figure 6 shows the sensitivity for the UV absorption profile at 1378 K. The UV absorption profile is very sensitive to the k_1 value. The change of k_1 value by a factor of 2 causes serious disagreement between the experimental and the modeling profiles. The proposed k_1 value is reliable within a factor of 2 at least below 1400 K.

We did not include the following isomerizations

$$2\text{-}C_4H_6 = 1\text{-}C_4H_6 \quad \text{(a6)}$$

$$1\text{-}C_4H_6 = 1,3\text{-}C_4H_6 \quad \text{(a7)}$$

in our mechanism. The inclusion of reaction a6 with the rate constant $k_{a6} = k_2$ predicts much more formation of 1-C_4H_6 (3.0% at 1200 K and 4.5% at 1300 K) than that observed. The inclusion of reaction a7 with the rate constant $k_{a7} = k_4$ predicted much more formation of 1,3-C_4H_6 in the pyrolysis of 1-C_4H_6 than that observed.[14] These isomerizations require more complicated H shifts (for example, simultaneous 1,3-H shifts of two H atoms) than those of reactions 1–4 and would be hard to occur. The experimental results can well be explained without reactions a6 and a7. However, if any, the maximum values which could account for the experimental data were $k_{a6} = (1/10)k_2$ and $k_{a7} = (1/10)k_4$.

There are other possible routes of the isomerizations of 2-C_4H_6 to 1,3-C_4H_6 and 1,2-C_4H_6. They are the following reactions:

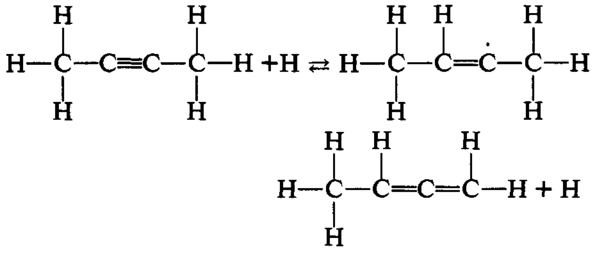

$$CH_3\text{—}C{\equiv}C\text{—}CH_3 + H \rightleftarrows CH_3\text{—}CH{=}\dot{C}\text{—}CH_3 \rightleftarrows CH_3\text{—}CH{=}C{=}CH_2 + H \quad \text{(a8)}$$

$$k_{a8} = (2.6 \times 10^5)T^{2.5} \exp(-1000\ \text{cal}/RT)\ \text{s}^{-1}$$
$$(=k_{10}, \text{assumed})$$

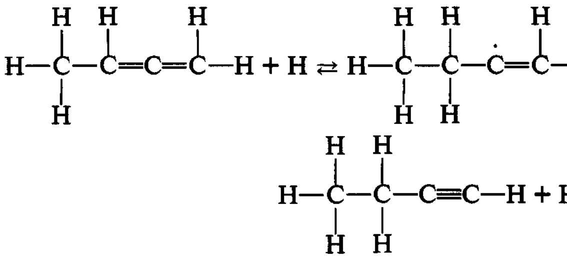

$$CH_3\text{—}CH{=}C{=}CH_2 + H \rightleftarrows CH_3\text{—}CH_2\text{—}\dot{C}{=}CH_2 \rightleftarrows CH_3\text{—}CH_2\text{—}C{\equiv}C\text{—}H + H \quad \text{(a9)}$$

$$k_{a9} = (6.0 \times 10^{12}) \exp(-2100\ \text{cal}/RT)\ \text{s}^{-1}$$
$$(=k_{12}, \text{assumed})$$

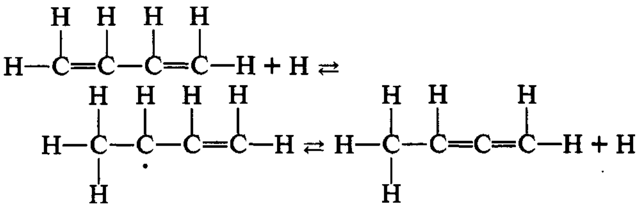

$$CH_2{=}CH\text{—}CH{=}CH_2 + H \rightleftarrows CH_3\text{—}\dot{C}H\text{—}CH{=}CH_2 \rightleftarrows CH_3\text{—}CH{=}C{=}CH_2 + H \quad \text{(a10)}$$

$$k_{a10} = (2.0 \times 10^{13}) \exp(-5000\ \text{cal}/RT)\ \text{s}^{-1}$$
$$(=k_{11}, \text{assumed})$$

When these reactions were added to the Table I mechanism, the computed yields of 1,3-C_4H_6 and 1,2-C_4H_6 and the remaining 2-C_4H_6 were slightly affected. The computed UV absorption profiles were also affected slightly by these reactions. When we eliminated reactions 1–4 and added reactions a8–a10, experimental data could not be reproduced at all. These facts mean that 2-C_4H_6 mainly isomerizes through reactions 1–4 and the isomerizations through reactions a8–a10 are not so important, at least at the initial stage of the reaction. In order to avoid complexity, we did not include reactions a8–a10 in our mechanism. The proposed rate constants k_1 and k_2 would, therefore, contain some contributions of reactions a8–a10.

General Features of the Reaction. In Figure 7 are shown the pR values[32] (logarithms of absolute values of net reaction rates in molecules cm^{-3} s^{-1} units) for the formation and the consumption of the C_4H_6 isomers. As is seen in this figure, most of the C_4H_6 isomers are consumed through three channels: (i) direct unimolecular decomposition of the C_4H_6 isomers (reactions 6–8); (ii) H atom addition to C_4H_6 isomers and subsequent decomposition of the adducts (reactions 10 and 11); (iii) abstraction of H atom from the C_4H_6 isomers by H, CH_3, and C_2H_3 and subsequent decomposition of the C_4H_5 isomers. Thus, the decomposition follows mainly a free-radical mechanism with the major chain carriers of CH_3 and H. The major initiation is reaction 6. The CH_3 radical is produced by reactions 6 and 10. The other major chain carrier, H atom, is mainly produced by reactions 35 and 68.

We can find out the route of the formation of major products from the pR values such as shown in Figure 7: CH_4 is mainly produced by reactions 21 and 22; C_2H_2 by reactions 8, 37, and 68; C_2H_4 by reactions 8, 11, and 27; propyne by reaction 10; vinylacetylene (C_4H_4) by reaction 35. Reaction 35 is not a single reaction, because H atom elimination from 2-C_4H_5 is expected to produce 1,2,3-butatriene ($^{\bullet}CH_2C{\equiv}CCH_3 \rightleftarrows CH_2{=}C{=}\dot{C}CH_3 \rightarrow CH_2{=}C{=}C{=}CH_2 + H$). We were, however, unable to find 1,2,3-butatriene. 1,2,3-Butatriene would rapidly isomerize to vinylacetylene. The other possible route of vinylacetylene formation from 2-C_4H_5 is the isomerization of 2-C_4H_5 to other C_4H_5 isomers and subsequent H atom elimination from the isomers.

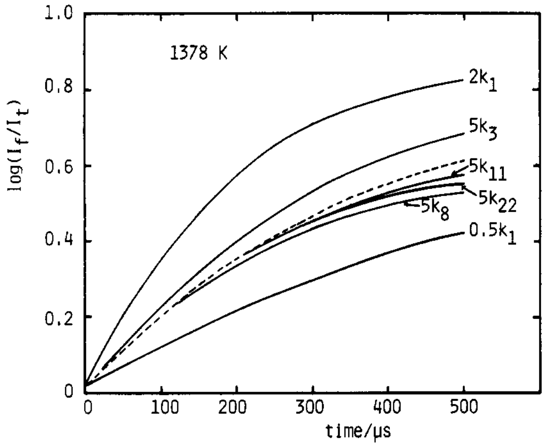

Figure 6. Sensitivity for the UV absorption profile at 230 nm. Conditions are the same as those of *C* in Figure 3. Broken line is computed with the Table I mechanism and rate constants. Solid lines are computed by multiplying the rate constants of Table I by 2 and 0.5 for k_1 and by 5 for others.

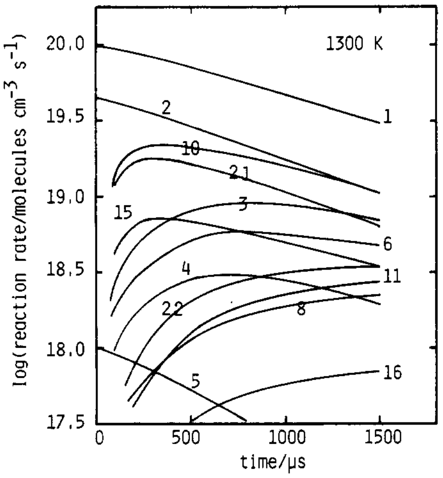

Figure 7. Reaction rate (p*R*) profiles at 1300 K for the 2.5% 2-C_4H_6–97.5% Ar mixture. Reactions which produce or consume C_4H_6 isomers are shown.

Conclusions

We found that 2-C_4H_6 rapidly isomerizes to 1,3-C_4H_6 and 1,2-C_4H_6 above 1100 K. We proposed the rate constants of these isomerizations and discussed the mechanism of the isomerizations. The proposed rate constants, k_1 and k_2, are applicable only at the total density of around 1.8×10^{-5} mol/cm^3, because our experiments are limited in the density range of 1.6×10^{-5} to 2.1×10^{-5} mol/cm^3. Theoretical studies will be needed to confirm the isomerization mechanism presented here.

The decomposition of 2-C_4H_6 is very complex, because of its very fast isomerization to 1,3-C_4H_6 and 1,2-C_4H_6. In order to understand the mechanism of 2-C_4H_6 decomposition, more experimental data for the decomposition of all the C_4H_6 isomers are needed.

References and Notes

(1) Skinner, G. B.; Sokoloski, E. M. *J. Phys. Chem.* **1960**, *64*, 1028.

(2) Kiefer, J. H.; Wei, H. C.; Kern, R. D.; Wu, C. H. *Int. J. Chem. Kinet.* **1985**, *17*, 225.

(3) Rao, V. S.; Takeda, K.; Skinner, G. B. *Int. J. Chem. Kinet.* **1988**, *20*, 153.

(4) Kiefer, J. H.; Mitchell, K. I.; Wei, H. C. *Int. J. Chem. Kinet.* **1988**, *20*, 787.

(5) Kern, R. D.; Singh, H. J.; Wu, C. H. *Int. J. Chem. Kinet.* **1988**, *20*, 731.

(6) Hopf, H.; Wachholz, G.; Walsh, R. *Chem. Ber.* **1985**, *118*, 3579.

(7) Cooper, W.; Walters, W. D. *J. Am. Chem. Soc.* **1958**, *80*, 4220.

(8) Frey, H. M.; Stevens, I. D. R. *Trans. Faraday Soc.* **1965**, *61*, 90.

(9) Srinivasan, R.; Levi, A. A.; Haller, I. *J. Phys. Chem.* **1965**, *69*, 1775.

(10) Hidaka, Y.; Nakamura, T.; Miyauchi, A.; Shiraishi, T.; Kawano, H. *Int. J. Chem. Kinet.* **1989**, *21*, 643.

(11) Hidaka, Y.; Oki, T.; Kawano, H. *Int. J. Chem. Kinet.* **1989**, *21*, 689.

(12) Hidaka, Y.; Masaoka, H.; Oshita, H.; Nakamura, T.; Tanaka, K.; Kawano, H. *Int. J. Chem. Kinet.* **1992**, *24*, 871, and references cited therein.

(13) Hidaka, Y.; Higashihara, T.; Ninomiya, N.; Oki, T.; Kawano, H. Manuscript in preparation.

(14) Hidaka, Y.; Higashihara, T.; Oki, T.; Kawano, H. Manuscript in preparation.

(15) Honjyou, N.; Pacansky, J.; Yoshimine, M. *J. Am. Chem. Soc.* **1984**, *106*, 5361. Honjyou, N.; Pacansky, J.; Yoshimine, M. *J. Am. Chem. Soc.* **1985**, *107*, 5332.

(16) Dean, A. M. *J. Phys. Chem.* **1985**, *89*, 4600.

(17) Fahr, A.; Laufer, A.; Klein, R.; Braun, W. *J. Phys. Chem.* **1991**, *95*, 3218.

(18) Hidaka, Y.; Higashihara, T.; Ninomiya, N.; Masaoka, H.; Nakamura, T.; Kawano, H. Manuscript in preparation.

(19) Koshi, M.; Fukuda, K.; Kamiya, K.; Matsui, H. *J. Phys. Chem.* **1992**, *96*, 9839.

(20) Hidaka, H.; Nakamura, T.; Tanaka, H.; Jinno, A.; Kawano, H.; Higashihara, T. *Int. J. Chem. Kinet.* **1992**, *24*, 761.

(21) Hidaka, Y.; Shiba, S.; Takuma, H.; Suga, M. *Int. J. Chem. Kinet.* **1985**, *17*, 441, and references cited therein.

(22) Frank, P.; Braun-Unkhof, M. *16th Symp. (Int.) on Shock Tubes and Waves, Aachen* **1987**, 379.

(23) Just, Th.; Roth, P.; Damm, R. *Symp. (Int.) Combust. [Proc.] 16th* **1976**, 961.

(24) Benson, S. W.; Haugen, G. R. *J. Phys. Chem.* **1967**, *71*, 1735.

(25) Hsu, D. S. Y.; Lin, C. Y.; Lin, M. C. *Symp. (Int.) Combust. [Proc.] 20th* **1984**, 623.

(26) Kiefer, J. H.; Mizerka, L. J.; Patel, M. R.; Wei, H.-C. *J. Phys. Chem.* **1985**, *89*, 2013.

(27) Tsang, W. In *Shock Waves in Chemistry*; Lifshitz, A., Ed.; Marcel Dekker: New York, 1981; p 60.

(28) Benson, S. W.; Cruickshank, F. R.; Golden, D. M.; Haugen, G. R.; O'Neal, H. E.; Rodgers, A. S.; Shaw, R.; Walsh, R. *Chem. Rev.* **1969**, *69*, 279. O'Neal, H. E.; Benson, S. W. *Int. J. Chem. Kinet.* **1969**, *1*, 221.

(29) Tsang, W. *Int. J. Chem. Kinet.* **1978**, *10*, 687.

(30) Ervin, K. M.; Gronert, S.; Barlow, S. E.; Gilles, M. K.; Harrison, A. G.; Bierbaum, V. M.; DePuy, C. H.; Lineberger, W. C.; Ellison, G. B. *J. Am. Chem. Soc.* **1990**, *112*, 5750.

(31) Wu, C. J.; Carter, E. A. *J. Am. Chem. Soc.* **1990**, *112*, 5893.

(32) Gardiner, W. C., Jr. *J. Phys. Chem.* **1977**, *81*, 2367.